0022-3565/10/3341-106–115$20.00
THE JOURNAL OF PHARMACOLOGY AND EXPERIMENTAL THERAPEUTICS
JPET 334:106–115, 2010

Vol. 334, No. 1
167882/3600670
Printed in U.S.A.

An Apolipoprotein E-Mimetic Stimulates Axonal Regeneration and Remyelination after Peripheral Nerve Injury

Feng-Qiao Li, Kenneth A. Fowler, Jessica E. Neil, Carol A. Colton, and Michael P. Vitek

Cognosci, Inc., Research Triangle Park, North Carolina (F.-Q.L., K.A.F., J.E.N., M.P.V.); and Division of Neurology, Duke University Medical Center, Durham, North Carolina (C.A.C., M.P.V.)

Received March 4, 2010; accepted April 19, 2010

ABSTRACT

Elevated apolipoprotein E (apoE) synthesis within crushed sciatic nerves advocates that apoE could benefit axonal repair and reconstruction of axonal and myelin membranes. We created an apoE-mimetic peptide, COG112 (acetyl-RQIKIWFQNRRMKWKKCLRVRLASHLRKLRKRLL-amide), and found that postinjury treatment with COG112 significantly improved recovery of motor and sensory function following sciatic nerve crush in C57BL/6 mice. Morphometric analysis of injured sciatic nerves revealed that COG112 promoted axonal regrowth after 2 weeks of treatment. More strikingly, the thickness of myelin sheaths was increased by COG112 treatment. Consistent with these histological findings, COG112 potently elevated growth associated protein 43 (GAP-43) and peripheral myelin protein zero (P0), which are markers of axon regeneration and remyelination, respectively. Electron microscopic examination further suggested that the apoE-mimetic COG112 may increase clearance of myelin debris. Schwann cell uptake of cholesterol-containing low-density lipoprotein particles was selectively enhanced by COG112 treatment in a Schwann cell line S16. Moreover, COG112 significantly promoted axon elongation in primary dorsal root ganglion cultures from rat pups. Considering that cholesterol and lipids are needed for reconstructing myelin sheaths and axon extension, these data support a hypothesis where supplementation with exogenous apoE-mimetics such as COG112 may be a promising strategy for restoring lost functional and structural elements following nerve injury.

Apolipoproteins have been implicated in the salvage and reutilization of myelin-derived cholesterol and lipids during Wallerian degeneration, subsequent nerve regeneration, and remyelination following peripheral nerve injuries (Skene and Shooter, 1983). Specifically, apolipoprotein E (*APOE*, gene; apoE, protein) was the most up-regulated protein after sciatic nerve crush, increasing several hundredfold (Ignatius et al., 1986) and then declining once regeneration is complete (Skene and Shooter, 1983). Macrophages that migrate into the injured tissue synthesize much of this apoE, which is released together with cholesterol and lipids derived from the degenerating myelin as a complex of cholesterol and apoE-containing lipoproteins. These lipoprotein particles are then taken up by low-density lipoprotein (LDL) receptors on the surface of Schwann cells (Mahley, 1988). All of these findings pointed to a significant role for apoE in neuroregeneration and remyelination. In support of this idea, enhanced neurite extension was observed upon the addition of apoE to rabbit dorsal root ganglion (DRG) cells cultured in vitro (Handelmann et al., 1992). Thus, strategies to stimulate the endogenous expression of apoE or the addition of an exogenous supply of reagents mimicking the function of apoE may prove to be beneficial in repairing damaged nerves.

There are three common isoforms of *APOE* in human populations, namely, *APOE2*, *3*, and *4*. In the last two decades, the *APOE4* allele was found to be a susceptibility factor for approximately 50% of all sporadic Alzheimer's disease

This work is supported in part by the National Institutes of Health National Institute of Neurological Diseases and Stroke [Grants NS052920, NS061392, NS058239]; the National Institutes of Health National Cancer Institute [Grant CA141819]; and the National Institutes of Health National Institute of Aging [Grant AG020473].

Article, publication date, and citation information can be found at http://jpet.aspetjournals.org.

doi:10.1124/jpet.110.167882.

ABBREVIATIONS: Antp, antennapedia; apoE, apolipoprotein E; DRG, dorsal root ganglion; GAP-43, growth-associated protein 43; LDL, low-density lipoprotein; LPS, lipopolysaccharide; LRP, low-density lipoprotein receptor-related protein; MS, multiple sclerosis; NGF, nerve growth factor; NO, nitric oxide; P0, peripheral myelin protein zero; PTD, protein transduction domain; SFI, sciatic functional index; TNF-α, tumor necrosis factor-α; TBI, traumatic brain injury; Fmoc, 9-fluorenylmethoxycarbonyl; PCR, polymerase chain reaction; ANOVA, analysis of variance; FBS, fetal bovine serum; PBS, phosphate-buffered saline; DMEM, Dulbecco's modified Eagle's medium; DiI, 3,3′-dioctadecylindocarbocyanine; IT, immediate treatment; DT, delayed treatment; COG112, (acetyl-RQIKIWFQNRRMKWKKCLRVRLASHLRKLRKRLL-amide); COG133, acetyl-LRVRLASHLRKLRKRLL-amide; COG112-DT, delayed treatment with COG112; COG112-IT, immediate treatment with COG112.

(Corder et al., 1993). The presence of *APOE4* also contributes to a poor clinical outcome in patients with stroke and traumatic brain injury (TBI) and multiple sclerosis (MS) compared with its *APOE3* counterpart (Corder et al., 1993; Chapman et al., 2001; Laskowitz and Vitek, 2007).

The difference between *APOE3* and *APOE4* in pathogenesis of neurological disorders might be related with their ability to modulate microglia, the primary cellular component of the innate immune response of the brain. Recently, we found that microglia derived from *APOE4/4*-targeted replacement mice demonstrated a proinflammatory phenotype that included altered cell morphology, increased nitric oxide (NO) production, and higher proinflammatory cytokine production, such as tumor necrosis factor-α (TNF-α) and interleukin-6, compared with microglia derived from *APOE3/3*-targeted replacement mice (Brown et al., 2002; Colton et al., 2002; Vitek et al., 2009). In addition, apoE exerts antioxidant, anti-inflammatory, antiexcitotoxic, and/or neurotrophic properties in an isoform-dependent fashion (Laskowitz et al., 1997; Aono et al., 2002; Colton et al., 2002). These properties of apoE, as well as its function in lipid and cholesterol transport, are mediated by specific receptors, such as the LDL receptors, the low-density lipoprotein receptor related protein (LRP), and scavenger receptors (Mahley, 1988).

To replicate the bioactivities of apoE holoprotein, a mimetic peptide was created from amino acid residues 133 to 149 located in the receptor-binding region of apoE protein (i.e., COG133, acetyl-LRVRLASHLRKLRKRLL-amide) that are not associated with the amino acid residues that distinguish apoE3 from apoE4. Similar to holo-apoE3 protein, COG133 inhibits lipopolysaccharide (LPS)-stimulated microglia activation, reduces TNF-α and NO production in vitro (Laskowitz et al., 2001), and suppresses brain and systemic inflammatory responses in LPS-injected mice (Lynch et al., 2003). Likewise, apoE-mimetic peptides retain the ability to bind LRP1 and other LDL receptors (Croy et al., 2004) and simulate the neuroprotective effect of apoE protein against *N*-methyl-D-aspartate excitotoxicity (Sheng et al., 2008). To enhance transmembrane permeability, COG133 has been molecularly modified by fusion with a protein transduction domain (PTD) derived from Drosophila antennapedia protein (Antp) to create COG112. This molecular fusion has been shown to greatly enhance the anti-inflammatory activity of COG133 in vitro and in vivo by use of an experimental autoimmune encephalomyelitis model of MS (Li et al., 2006). Therefore, we hypothesize that COG112, an improved analog of COG133, may demonstrate therapeutic efficacy in animal models of peripheral nerve injury by promoting functional recovery and tissue repair.

Materials and Methods

Experimental Procedures

Sequence and Synthesis of ApoE-Mimetic Peptides. The first generation apoE-mimetic peptide, COG133, is derived from residues 133 to 149 of human apoE (acetyl-LRVRLASHLRKLRKRLL-amide). COG112 is a chimeric peptide containing the antennapedia protein transduction domain RQIKIWFQNRRMKWKKC followed by COG133 (Li et al., 2006), resulting in a sequence of COG112 (acetyl-RQIKIWFQNRRMKWKKCLRVRLASHLRKLRKRLL-amide). All of the peptides were synthesized using standard Fmoc chemistries and purified by NeoMPS, Inc. (San Diego, CA) with a purity of >95%. Before use in animal experiments, the bioactivities of all peptides were confirmed by use of an in vitro screening model of LPS-induced release of inflammatory mediators (TNF-α and NO) from a murine microglia cell line, BV2.

Animal Surgery and Treatments. Eight-week-old female C57BL/6J mice were purchased from Charles River Laboratories (Raleigh, NC). The animals were maintained in the animal facility with controlled temperature and humidity at a 12/12-h light/dark cycle. Husbandry was in accordance with the Guideline of the Office of Animal Welfare of the National Institutes of Health with approved animal protocols by the Institutional Animal Care and Use Committee of Duke University. Before surgery, animals were anesthetized by intraperitoneal injection of anesthetic cocktail containing ketamine (50 mg/kg) and xylazine (10 mg/kg) and acepromazine (1 mg/kg). The left sciatic nerve at the mid-thigh region was exposed and crushed for 15 s two times with a 90° rotation between each crush using a hemostat clamped at the first setting as described previously (Goodrum et al., 2000). The sham control mice underwent surgery without crush. The muscle and skin were infused with antibiotics and then closed with 5/0 nylon sutures.

Immediately after crush surgery, mice were randomly assigned to one of the following treatment groups: 1) vehicle control, i.e., lactated Ringer's buffer; 2) peptide control Antp (1 mg/kg); 3) immediate treatment COG112 (1 mg/kg); and 4) delayed treatment COG112 (1 mg/kg). With the exception of the delayed treatment group where the treatment began 1 week after surgery, the other three groups were treated immediately after surgery by intraperitoneal injection on a daily basis for 2 weeks. Animals were sacrificed at the end of week 4 for histological and biochemical examination. In time-course experiments, animals were also sacrificed at 1 and 2 weeks after injury.

Functional Analyses

Walking Track Test. The analysis of an animal's walking pattern by recording its footprints is a widely used method for the assessment of motor nerve recovery (Bain et al., 1989). Footprints were recorded in a walking track (7.5 × 100 cm) with a darkened box at the end of the track. The floor of the corridor was covered with white paper. The hind paws were dipped in black ink so that they left paw prints as they walked. At least five consecutive footprints were taken for each hind paw. From the footprints, the following parameters were taken: distance from the third toe to the most posterior portion of the footprint or the print length; distance between the first and the fifth toes or the toe spread; and distance from the second to the fourth toe or the intermediary toe spread). All of the measurements of print length, toe spread, and intermediary toe spread were taken from both the nonoperated foot (NPL, NTS, and NIT, respectively) and the operated, experimental foot (EPL, ETS, and EIT, respectively). In the control animals, parameters of the right foot were compared with those from the left foot. The sciatic functional index (SFI) was calculated according to the following equation, adapted by Bain et al. (1989):

$$\mathrm{SFI} = -38.3\left[\frac{\mathrm{EPL} - \mathrm{NPL}}{\mathrm{NPL}}\right] + 109.5\left[\frac{\mathrm{ETS} - \mathrm{NTS}}{\mathrm{NTS}}\right] + 13.3\left[\frac{\mathrm{EIT} - \mathrm{NIT}}{\mathrm{NIT}}\right] - 8.8$$

where a value of SFI close to zero indicated normal nerve function, whereas approximately −100 implied total impairment.

Withdrawal Reflex Latency. The nociceptive response to thermal stimulation was assessed using a Plantar test apparatus (model 390; IITC Life Science, Woodland Hill, CA) according to the method of Hargreaves et al. (1988). Each mouse was placed in a clear plastic chamber (23 × 18 × 14 cm) and allowed to acclimate for 1 h before testing. A radiant heat source was positioned under the plantar surface of the hind paw to deliver a visible light beam at 20% active intensity. When the animal withdraws the paw, a button is pushed to

stop the heat source and the time is recorded. To prevent thermal injury, a cutoff time of 10 s was set. The mean paw withdrawal latency (in seconds) for the ipsilateral and contralateral hind paws was determined from an average of three separate measurements, with an interval of 30 min between consecutive tests to prevent sensitization phenomena. The difference in latency was calculated by subtracting the withdrawal latencies for the uninjured hind paw from the withdrawal latencies for the injured one. A positive "difference in latency" indicated thermal hypoalgesia, whereas a negative value implied thermal hyperalgesia.

Morphological Analyses

Another set of animals was used for histological study. The treatment paradigm and grouping are the same as above. Three animals were randomly selected and sacrificed at week 1, 2, or 4. After euthanasia, the distal portion of a crushed sciatic nerve was rapidly excised and immediately immersed in 4% formaldehyde, 2.5% glutaraldehyde (Sigma-Aldrich, St. Louis, MO) in 0.1 M phosphate buffer, pH 7.4, for 12 h at 4°C, keeping the specimen extended and oriented. After fixation, tissue samples were washed in phosphate buffer and postfixed for 90 min at room temperature in 1% osmium tetroxide (OsO_4; E.M.S., Hatfield, PA) and then dehydrated starting in an ethanol series and ending with propylene. Tissue samples were then embedded in a mixture of resins.

Light Microscopy. Semi-thin transverse sections (2-μm-thick) were cut at either 2 or 4 mm distal to the site of crush and stained with toluidine blue on glass slides. Sections were photographed at 600× with a Nikon microscope (TE2000) equipped with a Nikon digital camera (Nikon, Melville, NY). One section from each series was randomly selected and used for the morphometric-quantitative analysis performed using the NIH ImageJ software (version 1.40). For the quantitative analysis, a sampling square field, covering an area of 0.004 mm^2, was randomly positioned onto the selected digital image. In each sampling field, myelinated nerve fiber profiles were counted and measured by determining the outer and inner boundaries of the myelin sheaths by use of the automatic threshold tool. We used this method to collect the number of fibers, the fiber area, axon area, and the circle-fitting diameter of fibers (D) and axons (d). For each sampling region, we calculated the density of the fibers (number per millimeter squared, N/mm^2) and the myelin thickness $[(D - d)/2]$.

Transmission Electron Microscopy. Ultra-thin sections were cut immediately after the series of semi-thin sections using an Ultratome-III ultramicrotome (LKB, Bromma, Sweden). The sections were then photomicrographed using a JEM-1010 transmission electron microscope (JEOL, Tokyo, Japan) equipped with a Mega-View-III digital camera and a Soft-Imaging-System (SIS, Munster, Germany) for the computerized acquisition of the images.

Real-Time PCR

Nerve tissue used for mRNA analysis was extracted using freshly autoclaved RNase-free surgical tools. Sciatic nerves were excised from the site of crush to 5 mm distal and placed in RNase-free Eppendorf tubes containing RNAlater tissue RNA stabilization reagent (Qiagen, Valencia, CA) and stored at −80°C. Tissue homogenization was performed in TRIzol reagent (Invitrogen, Carlsbad) using trituration through 20-G needles. After chloroform extraction, the aqueous layer was further processed using the RNeasy column RNA purification kits from Qiagen. Reverse transcription was performed using the High-Capacity cDNA archive kit from Applied Biosystems (ABI 432271) in an Applied Biosystems 9700HT thermocycler (Applied Biosystems, Foster City, CA). Reverse transcriptase reactions were run at 25°C for 10 min, followed by 2 h at 37°C. Real-time PCR was performed using the TaqMan Gene Expression Assay Kit (Applied Biosystems) according to the manufacturer's instructions. In brief, cDNA samples (100 ng, based on the original RNA concentrations) were brought to a total volume of 22.5 μl using RNase-free water and mixed with 25 μl of 2× TaqMan Universal Master Mix and 2.5 μl of the respective 20× TaqMan Gene Expression Assay primers. Target amplification was performed in 96-well plates using a real-time sequence detection system instrument (ABI PRISM 7300HT; Applied Biosystems). The PCR thermal cycling conditions included an initial 10-min hold at 95°C to activate the AmpliTaq Gold DNA polymerase (Applied Biosystems), followed by 40 cycles of denaturation (15 s at 95°C) and annealing/primer extension (1 min at 60°C). The data from the real-time PCR experiments were analyzed using the $2^{-\Delta\Delta Ct}$ method, which allows for the calculation of relative changes in gene expression. For this method, the threshold cycle number (Ct) is normalized using a housekeeping gene (18S rRNA), calibrated to the control samples, and the result was used as the exponent with a base of 2 to determine the fold change in gene expression. Primers for these experiments were purchased from Applied Biosystems.

The Applied Biosystems identification number for each gene used is 18S (human eukaryotic 18S rRNA): Hs99999901_s1; growth-associated protein 43 (GAP-43) (murine growth-associated protein 43): Mm00500404_m1; and peripheral myelin protein zero (P0) (murine myelin protein zero): Mm00485139_m1. The information on exact primer sequences is available through the Applied Biosystems Web site.

Western Blotting

At 4 weeks after crush, sciatic nerves were excised from the site of crush to 5 mm distal. Nerves were extracted in lysis buffer containing a cocktail of proteinase and phosphatase inhibitors using a glass homogenizer. Protein lysate samples (30 μg) were resolved on 12.5% SDS-PAGE gels and transferred by electrophoresis to nitrocellulose membranes. The membrane was blocked at room temperature in PBS buffer containing 0.1% Tween 20 and 5% nonfat dried milk. Successively, the filters were cut, and the top was incubated overnight at 4°C alternatively with rabbit polyclonal antibody P0 (ab31851; Abcam Inc., Cambridge, MA) or rabbit polyclonal GAP-43 antibody (ab7462; Abcam Inc.). In parallel, the bottom filters were incubated with a primary rabbit polyclonal anti-α-tubulin antibody (ab59680; Abcam Inc.). Protein bands were detected using Li-Cor brand secondary fluorescent antibodies and visualized on the Li-Cor Odyssey infrared imaging system (LI-COR Biosciences, Lincoln, NE). The levels of protein expression for P0, GAP-43, and α-tubulin were calculated by measuring the peak densitometric area of the image acquired with a Li-Cor Scanner using Odyssey 2.1 software. To ensure that the fluorescent bands were in the linear range of intensity, different exposure times were used. The mean control value within a single experiment was set to 100, and all the other values were expressed relative to this control. Values of controls from different experiments were all within 10%.

LDL Uptake by Schwann Cells and Peritoneal Macrophages

S16 rat Schwann cell line was purchased from the American Type Culture Collection (ATCC, Manassas, VA) and grown in DMEM/10% FBS (Invitrogen). Cells were trypsinized and plated at a density of 2×10^5 per 12-mm poly-D-lysine-coated glass coverslip and allowed to adhere overnight. Cells were treated with 2 μg/ml DiI (3,3′-dioctadecylindocarbocyanine)-acetylated human LDL (Kalen Biomedical, LLC, Montgomery Village, MD) with or without 0.5 μM COG112 and COG133 peptides or controls for 4 h. After treatment, the coverslips were washed with 0.2 M acetic acid, pH 2.5, for 10 min to remove excessive extracellular labeled LDL. Coverslips were rinsed in PBS and fixed for 20 min in 4% formaldehyde/PBS before blocking for 30 min at room temperature in blocking buffer (10% normal goat serum/1% bovine serum albumin/0.1% Triton X-100). Coverslips were incubated overnight at 4°C with mouse anti-myelin-associated glycoprotein (mab1567; Millipore Corporation, Billerica, MA) diluted 1/10 in blocking buffer. Nuclei were labeled with

Hoechst dye 33342 before mounting in Vectashield Hard Mount (Vector Laboratories, Burlingame, CA). Images were quantified using ImageJ software.

DRG Culture

Isolated primary rat DRG from P2 Sprague-Dawley rat pups were mechanically dissociated with use of an 18-gauge needle before resuspending in culture media (DMEM/Neurobasal A, 1× B27 supplement, 0.5% FBS, penicillin/streptomycin, 10 ng/ml NGF). Cells were plated at 2×10^5 per 12-mm poly-D-lysine-coated glass coverslip. Treatment compounds were immediately added, and medium/compound was refreshed daily for 3 days. On day 3, coverslips were rinsed with PBS, fixed for 20 min with 4% formaldehyde in PBS, and blocked for 30 min (10% normal goat serum/1% bovine serum albumin/0.1% Triton X-100). Cells were stained overnight at 4°C with rabbit anti-neuron-specific beta III tubulin (ab18207; Abcam Inc.). ABC Elite horseradish-peroxidase kit (Vector Laboratories) was used to detect secondary biotinylated antibody and developed with 3,3′-diaminobenzidine (Vector Laboratories). Analysis was performed with use of Image-Pro Plus software (MediaCybernetics, Inc., Bethesda, MD).

Statistical Analyses

The data were analyzed using Prism (GraphPad Software, Inc., San Diego, CA). Two-way analysis of variance (ANOVA) was used to compare the behavioral, histological, and biological changes among treatment groups over time. One-way ANOVA was used to compare the means of the cell culture treatment groups. The data presented in graphs represent the mean ± S.E.M. (error bar).

Results

COG112 Promotes Functional Recovery in Mobility and Pain Sensation. Immediately after the acute compression injury, the crushed areas of all sciatic nerves were flattened; however, nerve continuity was not grossly interrupted. All animals demonstrated complete flaccid paralysis of the operative foot following crush injury. A variety of methods have been used to assay animal motor function and neural tissue repair after sciatic nerve injury. Footprint analysis is a widely used, noninvasive, and quantitative method that measures relationships between toes and feet of the animal's hind limb as expressed by an SFI (Bain et al., 1989). A value of SFI close to zero indicates normal nerve function, and a value of −100 implies total impairment. After crush injury, SFI of a vehicle control group ($n = 10$) decreased to 92.5 ± 8.9 at 1 week and then recovered progressively until the end of the experiment (data not shown). After 2 weeks, COG112 treatment had a significant effect (approximately 10% improvement) on the motor function of injured animals as revealed by an SFI score in comparison to vehicle control ($p < 0.01$) (Fig. 1A). In contrast, the control peptide Antp, which is the prefix peptide PTD of COG112, did not show a beneficial effect.

Because the treatment started immediately after crush injury, COG112 may also act in a therapeutic manner to prevent the secondary degeneration that follows the primary injury. To investigate whether COG112 exerts a therapeutic effect on secondary degeneration, a post-treatment paradigm was adopted. Animals were treated starting on day 8 after crush when Wallerian degeneration was mostly completed (Boyles et al., 1989; Goodrum, 1991). As shown in Fig. 1A, delayed treatment with COG112 also significantly improved recovery in motor function at the end of week 2 compared to vehicle controls, and there was no significant difference compared with the group with immediate COG112 treatment. It should be emphasized that the animals in the delayed treatment group received daily treatment for only 1 week, whereas the immediate treatment group was treated daily for 2 weeks. These data indicate that COG112 not only exerts a neuroprotective effect but also delivers a therapeutic effect to the injured peripheral nerves.

Sciatic nerve injury is usually accompanied with neuropathic pain (Ji and Suter, 2007). p38 Mitogen-activated protein kinase and TNF-α from macrophage/microglia play a significant role in the development of neuropathic pain states (Wagner and Myers, 1996; Ji and Suter, 2007). Because COG112, as well as other apoE-mimetics, potently inhibit microglia activation and inflammatory cytokine release both

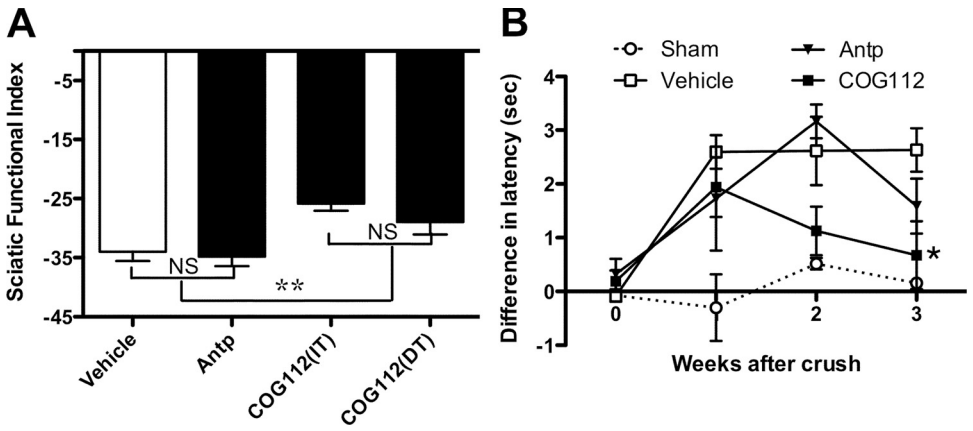

Fig. 1. COG112 treatment promotes motor and sensory recovery in mice following sciatic nerve crush. C57BL/6J female mice received IT by daily intraperitoneal injection of vehicle, negative control peptide Antp (1 mg/kg), or COG112 (1 mg/kg) for 2 weeks. Another group of animals received DT with COG112 (1 mg/kg) in which treatment was not started until day 8 (1 week after injury) and treatment continued for 2 weeks (weeks 2 through 3). A, comparison of SFI among treatment groups 2 weeks after injury. Footprints were recorded by dipping the hind paws in black ink and allowing them to walk in a confined walkway lined with white paper on the bottom. SFI is calculated using the formula as described under *Materials and Methods*. Animals received IT or DT of COG112, and both significantly improved SFI score compared with vehicle or Antp negative-control group (**, $p < 0.01$). There is no significant difference between the IT and DT groups. B, pain sensation was measured by Plantar test apparatus using Hargreave's method and expressed as difference of paw withdrawal latency (in seconds) from the injured side and the noninjured side of each individual animal. Only the group receiving COG112 (1 mg/kg for 2 weeks intraperitoneally) significantly recovered from pain sensation following sciatic nerve injury compared with vehicle controls (*, $p < 0.05$). The experiment was repeated three times, and the results were consistent.

in vitro and in vivo (Lynch et al., 2003; Li et al., 2006), we conducted experiments to determine whether COG112 modulates pain after sciatic nerve injury. The nociceptive response to thermal stimulation was assessed weekly for 2 weeks with use of a Plantar test apparatus according to the method of Hargreaves et al. (1988). The latency of paw withdrawal response was measured from both hind limbs (injured side and noninjured side), and the difference in paw withdrawal latency was calculated by subtracting the latency of the injured side from that of the noninjured side. Crush procedure induces an evident pain sensation after injury that persists for at least 2 weeks in the vehicle control group. As shown in Fig. 1B, treatment with COG112 significantly lowered the thermal threshold at week 2 compared with the vehicle group ($P < 0.05$), even though it did not counteract the injury-induced neuropathic hyperalgesia at 1 week. These data together suggest that the apoE-mimetic COG112 was able to promote functional motor and sensory recovery after peripheral nerve injury.

COG112 Treatment Significantly Promotes Axonal Regeneration and Remyelination In Vivo. The presence of functional recovery usually indicates histological repair. To investigate whether COG112 treatment affected the process of axon regeneration and remyelination, three animals from each group were randomly selected for histological examination of sciatic nerves at different time points, i.e., 1, 2, and 4 weeks after surgery. Figure 2A demonstrates a normal appearance of the sciatic nerve from sham control animals, with small and large diameter myelinated fibers regularly distributed. One week after crush injury, most of the myelinated and unmyelinated fibers were undergoing severe dystrophy in all animals, regardless of treatment. However, in COG112-treated animal, there were still some myelinated axons as shown in Fig. 2D. Two weeks after nerve crush, early axonal regeneration and myelination were evident in all treatment groups, but there were myelinated axon fibers in the COG112-immediate treatment group (Fig. 2H), whereas there were more debris-loaded macrophages in both vehicle and control peptide (Antp)-treated animals. Four weeks after injury, axonal regeneration became more advanced as depicted in Fig. 2, I to L. Although recovery had not achieved the level of the sham control, immediate treatment with COG112 (COG112-IT) demonstrated the most advanced state of axonal regeneration at 2 and 4 weeks after injury. As shown in Fig. 2, H and L, larger diameter axons with lower fiber densities and thicker myelin sheaths were found in this treatment group compared with the other groups. Delayed treatment with COG112 (COG112-DT) shows similar regenerative improvements such as COG112-IT but does not appear to be as effective. Both treatments, however, were improved compared with either vehicle or Antp-treated control animals.

To quantify the extent of axonal regeneration and myelination between control groups and COG112-treated groups, we carried out a morphometric analysis of myelinated fibers at 1, 2, and 4 weeks after nerve crush. The number of myelinated axons was counted in each microscopic field of 400 μm^2 (20×20 μm). One week after sciatic nerve injury, the distal segments 2 mm from the crushed site displayed almost complete degeneration, as shown by >98% reduction in axon density in the vehicle control group compared with the sham control (Fig. 3A). To some extent, immediate treatment with COG112 preserves some axons from degeneration within the 1st week, as shown by the approximately 2-fold higher axon density in the COG112 group compared with vehicle controls ($p < 0.01$; Fig. 3A). Two weeks after injury, the density of axonal fibers in all treatment groups is dramatically increased, with axon density in the COG112-IT group being

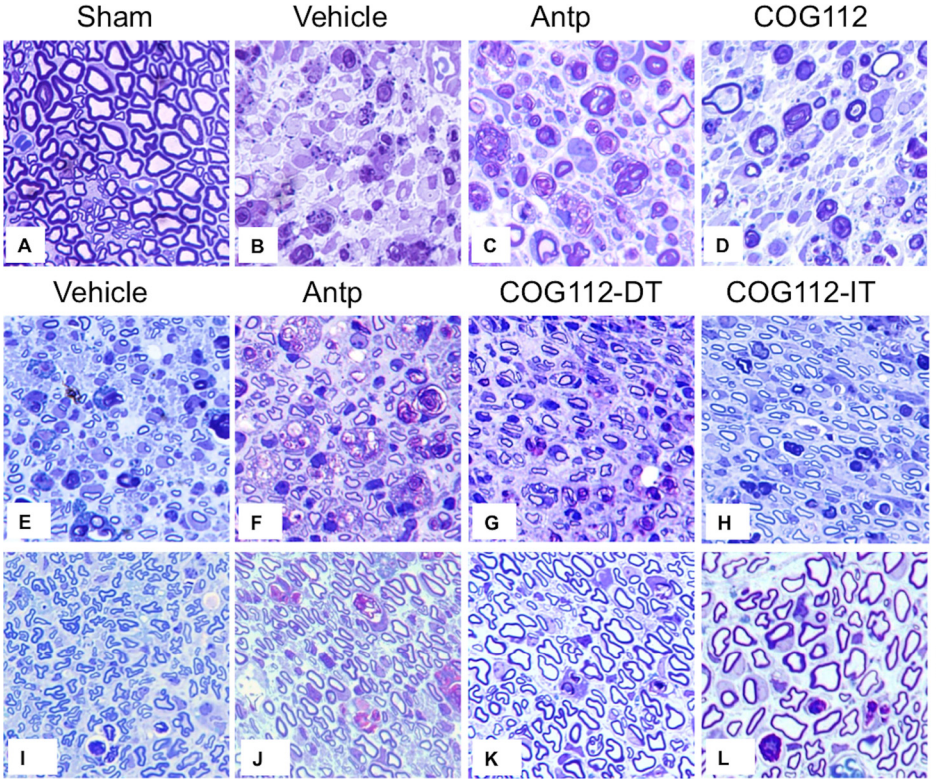

Fig. 2. Representative light microscopic photographs of regenerating and remyelinating nerves in mice following sciatic nerve crush. Semi-thin coronal sections, 2 mm distal to the crushed site, were collected and cut from different treatment groups at 1, 2, or 4 weeks after sciatic nerve crush and stained with toluidine blue. A, normal appearance of sciatic nerve, with small and large diameter myelinated fibers regularly distributed, in the sham group. B to D, the dystrophy appearance of injured nerves 1 week after crush injury is evident in all treatment groups. In the COG112-treated group, some existing axons can still be sporadically found, whereas they are rarely found in vehicle or Antp-treated group. E to H, axon regeneration and myelination start and appear to be more advanced in both COG112 groups. I to L, 4 weeks after nerve crush, there are more thinner axon fibers in both vehicle and control peptide (Antp) groups, suggesting a less advanced status of axon regeneration compared with COG112 groups. COG112-IT group demonstrates lower density of fibers but larger axon diameters than the COG112-DT group. Magnifications: 600×.

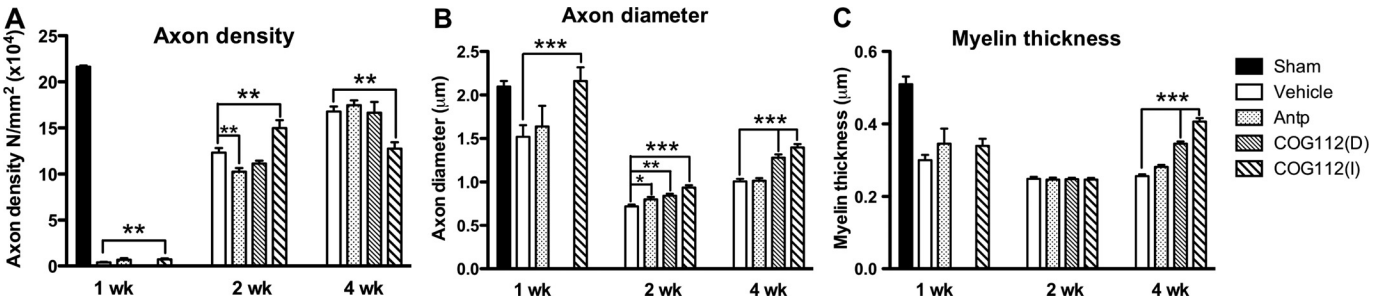

Fig. 3. Major parameters of axon maturation in sciatic nerves 1, 2, or 4 weeks after injury. A, the numbers of myelinated axons were counted in each field of 0.004 mm^2. B and C, both the axon (inner circle, B) and fiber (outer circle) diameters were measured using the NIH ImageJ software, and the myelin thickness (C) was calculated. Data are presented as mean ± S.E.M. Multiple group comparison was conducted by one-way ANOVA followed by post-hoc Newman Keuls Multiple Comparison Test with use of Prism software (version 5). *, $p < 0.05$; **, $p < 0.01$; ***, $p < 0.001$. COG112(D), delayed treatment with COG112; COG112(I), immediate treatment with COG112.

significantly higher than the other groups, including the COG112-DT group (Fig. 3A). However, the animals in COG112-DT group received COG112 treatment for a total of only 1 week at the end of 2 weeks after crush and, thus, represents only half of the treatment duration as that of the other groups. Compared with almost complete degeneration at 1 week after injury, the robustly increased axon density at 2 weeks indicates an axonal regeneration occurrence between 1 and 2 weeks, and treatment with COG112 seems to promote this regeneration ($p < 0.01$, COG112-IT versus vehicle group; Fig. 3A).

As depicted in Fig. 2, newly regenerated axons are also characterized by smaller fibers, i.e., smaller axon diameters compared with normal axons (Fig. 3B). By inspection and measurement at 2 weeks, the axon diameter in the COG112-IT group is significantly larger than that of other groups, suggesting a more mature status of axon regeneration in response to COG112 treatment at this time point. However, there is no difference in myelin thickness among all treatment groups at this moment (Fig. 3C). Four weeks after sciatic nerve injury, there was a significant increase in the numbers of myelinated axons in all of the treatment groups. However, in the COG112-IT group, there was a significantly lower axon density with a higher axon diameter, indicating a more matured axonal regeneration (Mazzer et al., 2008). Even in the COG112-DT group, the mean axon diameter is significantly larger than either the vehicle control or Antp control group ($p < 0.001$; Fig. 3B). As depicted in Fig. 3C, the most significant change at 4 weeks is that COG112 treatment potently increased the myelin thickness compared with the control groups ($p < 0.001$). Taken together, COG112 robustly boosts both axonal regeneration and remyelination.

COG112 Increases GAP-43 and P0 Gene Expression and Protein Synthesis in Sciatic Nerve after Injury. In addition to the histological evidence shown above, we measured the levels of GAP-43 and P0, biomedical markers of regeneration and remyelination, respectively. GAP-43 is an intracellular growth-associated protein mostly expressed in the growth cone of axons that appears to assist axonal pathfinding and branching during development and regeneration (Denny, 2006). Therefore, GAP-43 has been considered to be a good marker of axonal growth. P0 is the main myelin protein of peripheral nerves and represents 50 to 70% of total myelin protein. The 28-kDa glycoprotein is only expressed in myelinating Schwann cells and is not expressed in nonmyelinating Schwann cells or central nervous system glia (Garbay et al., 2000). Therefore, the level of P0 protein is clearly associated with remyelination following sciatic nerve crush (Song et al., 2006).

We used real-time PCR to measure the levels of GAP-43 and P0 in isolated sciatic nerves at specific time points after injury. The effects of immediate treatment with COG112 for 2 weeks were then compared with vehicle and Antp-only controls at the same time points. GAP-43 mRNA levels were increased by 1 week after injury under all conditions. However, by 2 weeks of treatment, COG112 robustly augmented the expression of GAP-43 (Fig. 4A, $p < 0.001$ compared with vehicle and Antp controls). In contrast, gene expression of P0 in the distal segment was reduced significantly at 1 week after sciatic nerve injury in all groups. Similar to GAP-43, 2 weeks of treatment with COG112 resulted in a significant increase in P0 mRNA levels (Fig. 4B). Treatment was then stopped, and mRNA and their corresponding protein levels were measured after 2 additional weeks (2 weeks of treatment plus 2 weeks of recovery, 4 weeks total). Cessation of treatment after 2 weeks followed by an additional 2 weeks of recovery resulted in decreased mRNA for GAP-43 in COG112-treated mice by 4 weeks after injury (Fig. 4A). However, protein levels for GAP-43 remained elevated at this same 4-week time point (Fig. 4C). P0 mRNA and protein levels remained elevated throughout the additional 2 weeks compared with both of the control groups (Fig. 4, B and D).

The protein level of GAP-43 and P0 was quantified by Western blotting 4 weeks after injury. As depicted in Fig. 4, C and D, the protein level of both GAP-43 and P0 in the COG112 treatment group is significantly higher than that of animals receiving vehicle or Antp treatment. Thus, the changes induced by treatment persisted for at least 2 additional weeks after cessation of COG112 treatment.

COG112 Promotes Axon Growth in Primary DRG Cultures. Primary DRG culture is a frequently used in vitro model for investigation of various agents on neurite outgrowth and/or neuroregeneration. To further confirm the effect of COG112 on axon regeneration seen in whole animals, primary DRG cultures from P2 Sprague-Dawley rat pups were treated with COG112 (0.1 μM), Antp (0.1 μM), COG133 (1 μM, not shown), or NGF (2.5S, 200 ng/ml) for 5 days. Figure 5, left, shows that COG112 significantly stimulates axonal elongation, which is comparable with that of NGF-treated cultures. Axonal length (the longest axon of each neuron) was measured using Image-Pro Plus software, and the quantitative data are presented in the right panel. Both

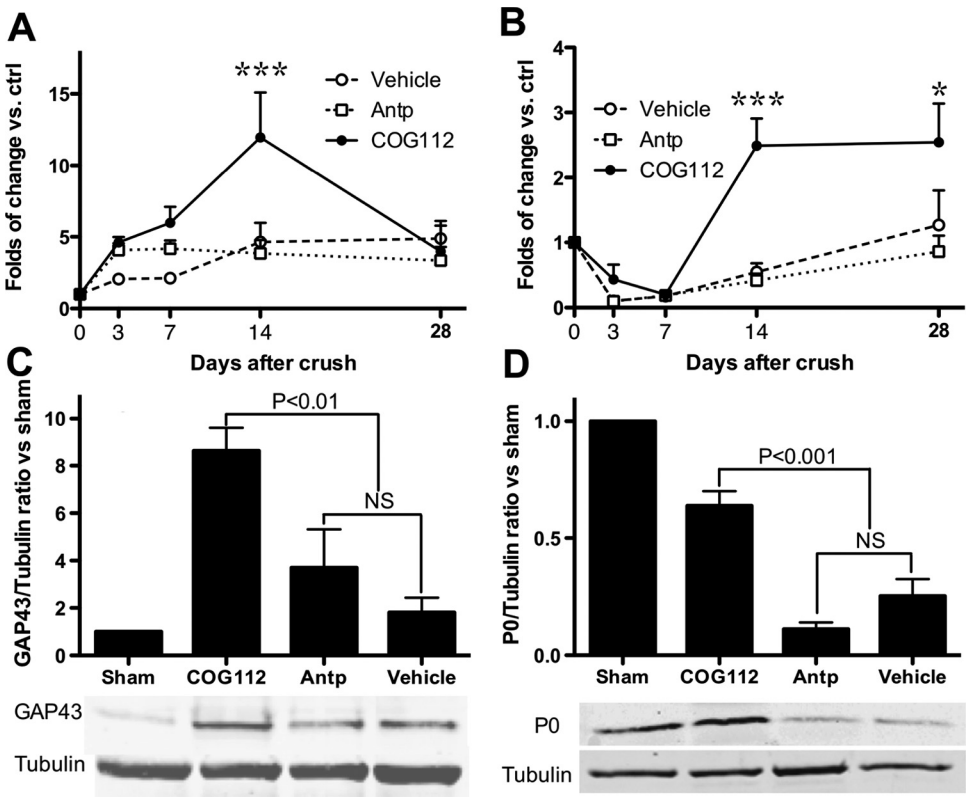

Fig. 4. COG112 treatment increases gene expression of GAP-43 and P0 by real-time PCR (A and B) and protein synthesis by Western blotting (C and D). Sciatic nerve crush was conducted on C57BL/6 mice on day 0. The animals received treatment with COG112 (1 mg/kg) or Antp (1 mg/kg) or vehicle control by intraperitoneal injection immediately after crush injury and then followed by daily dosing. Animals were sacrificed on day 3, 7, 14, or 28 for real-time PCR examination of GAP-43 (A) and P0 (B) gene expression. Each time point represents the mean ± S.E.M. (n = 3–9) after normalization with 18S rRNA. Two-way ANOVA resulted in a significant effect of treatment ($P < 0.05$). The results of the post-hoc Tukey-Kramer test are indicated as follows: *, $p < 0.05$; ***, $p < 0.001$ versus vehicle control. C and D, protein synthesis of GAP-43 (C) and P0 (D) after treatment for 2 weeks (first 2 weeks) and after 4 weeks after crush injury by Western blotting. Eight mice were used for each group. Because of the small size of sciatic nerve, two of them from the same treatment group were combined to obtain enough lysate protein for Western blotting. The columns represent the means ± S.E.M. (n = 4) after normalization with α-tubulin. One-way ANOVA resulted in a significant effect of treatment ($p < 0.001$) and by post-hoc Tukey-Kramer test: NS, not significant; **, $p < 0.01$; ***, $p < 0.001$ compared with vehicle control.

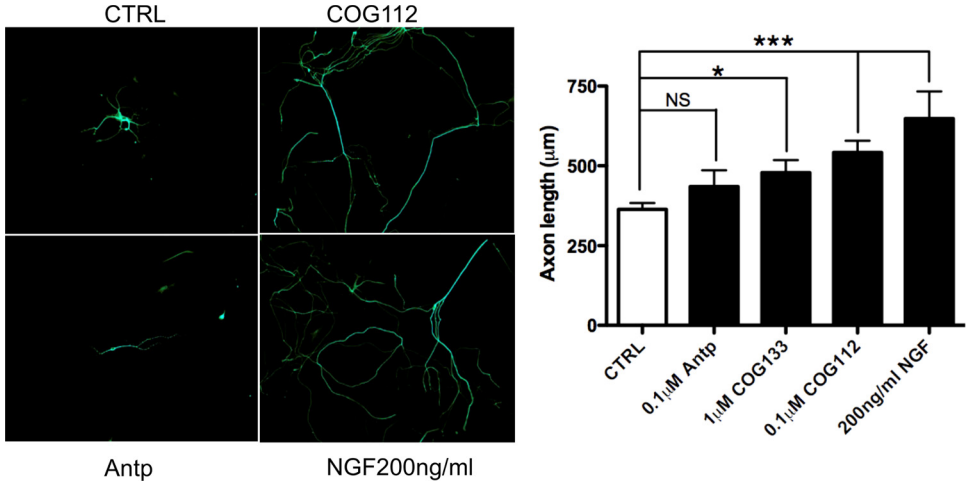

Fig. 5. COG112 stimulates neurite outgrowth from cultured DRG neurons. Left, the representative examples of primary DRG neurons from P2 Sprague-Dawley rat pups after treatment with either COG112 (0.1 μM) or Antp (0.1 μM), COG133 (1 μM, not shown) or NGF (2.5S, 200 ng/ml) for 5 days. On day 5, cells on coverslips were stained overnight with primary antibody TUJ1 (Abcam Inc.), followed by secondary antibody for 1 h (Alexa Fluor 488; Invitrogen). Axonal length (the longest axon of each neuron) was measured using Image-Pro Plus software, and the quantitative data were presented in adjacent graph. The columns present axonal length as means ± S.E.M. ANOVA analysis followed by post-hoc Newman Keuls test was used to compare the differences among groups. NS, not significant; *, $p < 0.05$; ***, $p < 0.001$ versus control.

COG112 and NGF-treated cultures bear significantly longer axons compared with untreated cultures ($p < 0.001$), whereas COG133 mildly enhances the neurite extension ($p < 0.05$). These data indicate that apoE-mimetics exert neurotrophin-like effects on axon growth in primary DRG cultures.

COG112 Increases Uptake of LDL by Schwann Cells. Schwann cells are the myelinating cells in the peripheral nervous system. Because we have found that COG112 potently promotes remyelination of sciatic nerves after crush injury, we postulate that COG112 may partially enhance Schwann cell-mediated repair through an increased supply of cholesterol and lipids, which are required for efficient remyelination. First, cross-sections of sciatic nerve 2 mm distal to the injured site were examined by electron microscopy at 2 weeks after injury. As depicted in Fig. 6, although there is no visible difference in myelin thickness between vehicle or COG112-treated animals, there are obviously more Schwann cells intensively loaded with lipid droplets in the COG112-treated animals compared with their vehicle controls, suggesting that COG112 can facilitate the uptake of myelin debris by Schwann cells. Because apoE has been associated with the recycling and reutilization of myelin debris (Boyles et al., 1989; Goodrum, 1991), these current data indicate that apoE-mimetic peptide may replicate this aspect of apoE holoprotein function.

To further confirm the uptake seen in the crush model of regeneration, we investigated the effect of apoE-mimetics on the uptake of LDL by the S16 Schwann cell line. As demonstrated in Fig. 7, COG112 specifically and dramatically increases the uptake of acetylated human LDL by

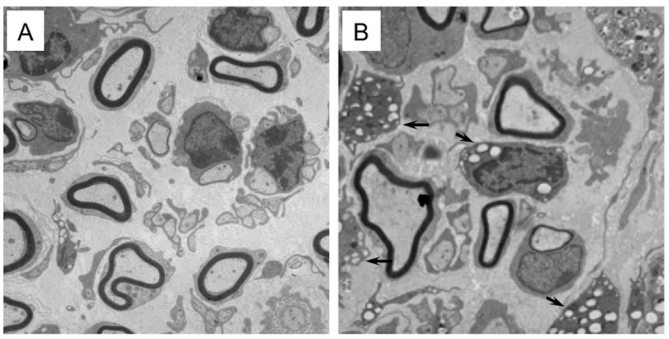

Fig. 6. Electron microscopic photographs of sciatic nerves 2 weeks after injury. A, vehicle control mouse. B, COG112-IT mouse. Although remyelination had started and there is no clear difference between these two groups at this point in time, there are clearly more macrophages loaded with lipid droplets (arrows) in COG112-treated animals. Three animals were examined from each group, and similar results were observed in each case. Magnifications: 3000×.

S16 Schwann cells compared with either PBS control or the mixture of COG113 and Antp ($p < 0.001$). It is surprising that COG112 does not affect the uptake of LDL by peritoneal macrophages. Although clearance of axonal and myelin debris has been attributed to the cooperative actions of both macrophage and Schwann cell following Wallerian degeneration, Schwann cells are capable of substantial myelin degradation unaided by macrophages as demonstrated by Fernandez-Valle et al. (1995). Given that acetylated LDL contains a substantial amount of cholesterol and lipids, increased uptake of LDL by COG112 may facilitate the supply of cholesterol and lipids for regenerative Schwann cells where both are required for myelin reconstruction. Thus, enhanced uptake of LDL by COG112 may be important for clearing the inhibitory debris and to allow subsequent regeneration.

Discussion

The robust relationship between apoE and peripheral nerve degeneration/regeneration was established over 20 years ago, making apoE an ideal candidate as a therapeutic target for the treatment of peripheral neuropathy (Skene and Shooter, 1983; Boyles et al., 1989; Nathan et al., 1994). Until now, this concept has not been successfully translated into a therapeutic approach. Our data strongly suggest that an apoE-derived mimetic strategy can potentially stimulate both axon regeneration and remyelination, as well as promote functional recovery following peripheral nerve injury. The strategy circumvents the problems of apoE as a large protein that does not readily cross the blood-brain barrier. Furthermore, molecular modification to the original apoE-mimetic peptide (COG133) by fusion with a PTD results in significantly improved permeability of the blood-brain barrier and enhanced bioactivities both in vitro and in vivo (Li et al., 2006; Singh et al., 2008).

The therapeutic efficacy of apoE-mimetics has been previously demonstrated in multiple animal models of a variety of neurological disorders, including TBI, MS, and subarachnoid hemorrhage (Lynch et al., 2005; Gao et al., 2006; Li et al., 2006). These beneficial effects are mostly associated with its neuroprotective activities. In the present study, immediate treatment with COG112 rendered better tissue protection by 2 weeks after injury compared with delayed treatment in which the treatment was not initiated until complete degeneration had developed (by 1 week after injury). Therefore, the overall outcome of COG112 treatment may come from a combination of both neuroprotective and neuroreparative effects.

Multiple mechanisms may be involved in the neuroprotective effect of apoE-mimetics. It has previously been shown

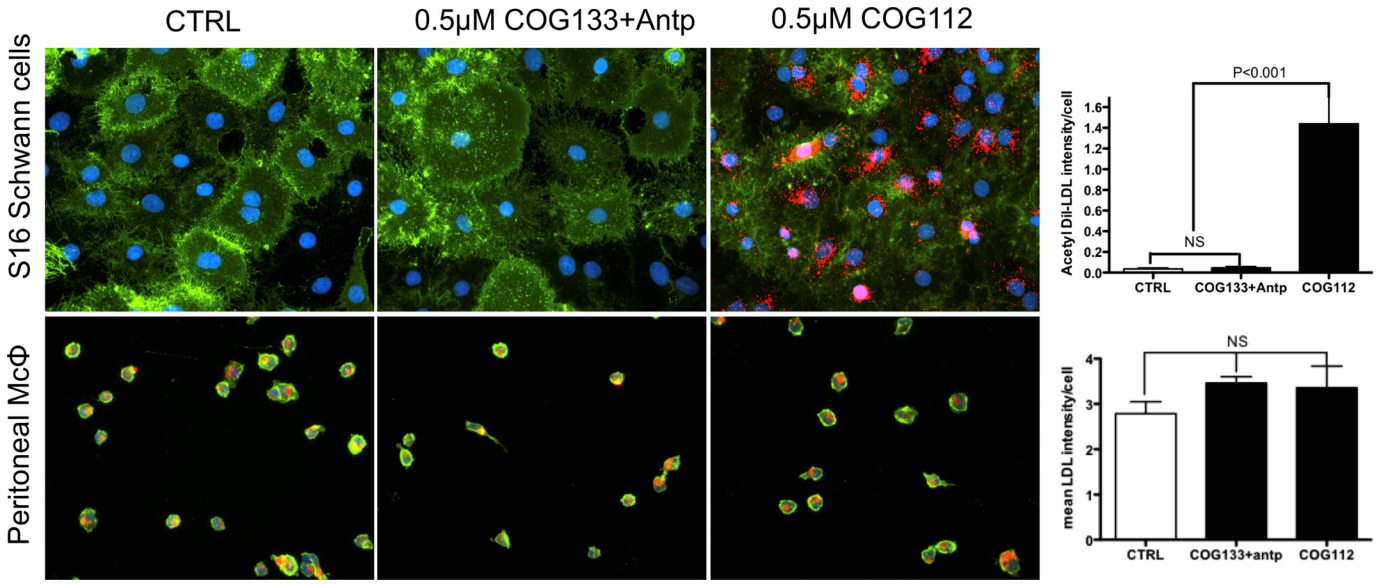

Fig. 7. ApoE-mimetic COG112 enhances the uptake of acetylated LDL by Schwann cells in vitro. Top row, S16 rat Schwann cell line was grown in DMEM/10% FBS (Invitrogen) at a density of 2×10^5 per 12-mm poly-D-lysine-coated glass coverslip. Bottom row, peritoneal macrophages were collected from adult Sprague-Dawley rats through peritoneal lavage. Cells were treated with 2 μg/ml DiI-acetylated LDL (Kalen Biomedical, LLC) with or without 0.5 μM COG112 and COG133 peptides or control for 4 h. The coverslips were washed with 0.2 M acetic acid to remove excessive extracellular labeled LDL. After fixation for 20 min in 4% formaldehyde/PBS, the cell structure was visualized by labeling with myelin-associated glycoprotein antibody for S16 or Mac-2 for macrophages with Hoescht dye 33342 for nuclei. Images were captured with Nikon Ti-S inverted microscope equipped with Nikon DS-Qi1 monochrome quantitative camera. The uptake of LDL was quantified by measuring the fluorescence intensity of DiI (in red) within the cytoplasm using NIS-Elements software (Nikon Instruments Inc., Melville, NY). COG112 treatment resulted in significantly greater uptake of acetyl-LDL by Schwann cells than by macrophages. Statistical analysis was conducted with GraphPad Prism software. Magnification: 400×.

that the apoE-mimetic COG133 is anti-inflammatory in nature and can improve outcome following TBI (Lynch et al., 2005; Laskowitz and Vitek, 2007). Our second generation mimetic, COG112, was found to be more potent in anti-inflammatory activity, and a large part of the neuroprotective properties of COG112 may be mediated via this mechanism (Li et al., 2006; Singh et al., 2008). Because acute inflammatory responses are generally considered to be beneficial in nerve injury due to the requirement for recruiting macrophage to the injured site to clear degraded debris, the use of an anti-inflammatory may seem paradoxical. However, sustained chronic inflammation is detrimental for the functional recovery following peripheral nerve injury (Kato et al., 2002; Gaultier et al., 2008). Peripheral nerve injury and neuropathic pain are associated with changes in proinflammatory cytokine expression in the superficial dorsal horn of the spinal cord (Ji and Suter, 2007). In peripheral nervous system injury, TNF-α plays a principal role in orchestrating many of the events involved in Wallerian degeneration and sensitizing nociceptors (Sorkin et al., 1997). In fact, neuropathic pain states have been modeled by direct administration of TNF-α into uninjured sciatic nerves (Wagner and Myers, 1996). Given that COG112 is one of the most potent apoE-mimetics in reducing TNF-α production, inhibition of TNF-α may be instrumental for the ability of COG112 to attenuate the pain response following sciatic nerve crush, to preserve Schwann cells, and to promote tissue repair (Kato et al., 2002; Gaultier et al., 2008). Another protective mechanism is related to glutamate excitotoxicity. Both apoE protein, as well as its mimetic peptide COG133, can prevent primary neurons from excitotoxicity-induced calcium influx and subsequent cell death (Aono et al., 2002, 2003) through binding to the low-density lipoprotein receptor-associated protein (Sheng et al., 2008). A similar protective effect of COG112 was recently validated by our laboratory (F.-Q. Li and L. Chen, manuscript in preparation).

Beyond neuroprotection, this study presents a novel property of an apoE-mimetic in neurorestoration, including neuroregeneration and remyelination. In the present study, we show three lines of evidence indicating enhanced regeneration and remyelination by COG112 in a sciatic nerve crush model. Histological staining revealed 1) increased axon density at 2 weeks after crush and increased axon diameter and myelin thickness at 4 weeks after crush; 2) increased gene expression (by real-time PCR) and protein synthesis (by Western blotting) of biomarkers of regeneration and remyelination, i.e., GAP-43 and P0, respectively, following treatment with COG112; and 3) enhanced axon extension in primary DRG cultures. COG112 dose-dependently promotes axonal elongation, similar to the effect of NGF (Fig. 5), suggesting that apoE-mimetics may possess neurotrophin-like activity. It has been known that apoE protein exerts neurotrophic effects in an isoform-dependent manner, i.e., apoE3 is more efficient than apoE4 in promoting neurite outgrowth (Nathan et al., 1994). There is already direct evidence that apoE-containing lipoproteins can influence both lipoprotein uptake as well as neurite outgrowth in vitro (Handelmann et al., 1992). ApoE also binds to and potentiates the biological activity of ciliary neurotrophic factor (Gutman et al., 1997). From these reports, it seems clear that apoE has important functions in maintaining neuronal integrity and survival. The present study, for the first time, shows that apoE-mimetic peptides exert a neurotrophic effect similar to that of apoE holoprotein. It is noteworthy that apoE-mimetic peptides retain binding affinity to LRP1 (Croy et al., 2004). Most recently, a shed form of LRP1 was found to promote functional and histological recovery from peripheral nerve injury (Gaultier et al., 2008). We hypothesize that binding to LRP may be instrumental for the neurotrophic effect of COG112 seen in this study.

ApoE-mimetics may also contribute to a more permissive environment that allows axonal regeneration and remyelination at the injury site. After a denervating crush injury, large amounts of lipid are released from degenerating axon membranes and myelin. Much of the cholesterol from these membranes becomes associated with lipoproteins containing apoE and is stored by cells in the nerve bundle for reuse during regeneration (Goodrum, 1991). Thus, during nerve degeneration and regeneration, apolipoproteins, such as apoE and apoA-I, and the LDL receptor could play a role in facilitating cholesterol movement both into and out of cells (Goodrum et al., 2000). In support of this hypothesis, apoE was found to be the most highly expressed protein following sciatic nerve injury (Boyles et al., 1989), which is spatially and temporally matched with the process of axonal regeneration (Skene and Shooter, 1983; Müller et al., 1985). Once regeneration is complete, apoE levels decline (Müller et al., 1985). Together, these data suggest that apoE may play an essential role during axonal regeneration by facilitating the clearance of myelin debris and enhancing reutilization of cholesterol and lipids.

In the peripheral nervous system, clearance of axonal and myelin debris has been attributed to the cooperative actions of two cell types, the indigenous Schwann cells and the macrophages recruited to the regions of tissue damage (Fernandez-Valle et al., 1995). Electron-microscopic examination showed that numerous lipid droplets from axon and myelin degeneration had already accumulated within Schwann cells and macrophages by 3 days after injury (Boyles et al., 1989). Although macrophages are thought to play an important role in myelin degradation during Wallerian degeneration, there is also evidence that Schwann cells carry out degradation of short myelin segments and proliferate without macrophage assistance during Wallerian degeneration (Fernandez-Valle et al., 1995). Thus, Schwann cells not only function as myelin-ensheathing cells but also may act like macrophages. In contrast, cholesterol from degenerating myelin that is salvaged by macrophages needs to be resupplied to myelinating Schwann cells with the assistance of lipoproteins, including apoE. It is likely that enhanced uptake of lipid and cholesterol directly by Schwann cells might be a more efficient way for myelin to be reconstructed. Thus, the increased LDL uptake observed with COG112 treatment suggests that COG112, as a mimetic of apoE, does replicate the function of its holoprotein. Specifically, COG112 increases the uptake of LDL by Schwann cells, providing an interpretation for the enhanced remyelination following COG112 treatment in the whole animal model of peripheral nerve injury.

The mechanism governing how apoE-mimetics affect lipid uptake specifically by Schwann cells will require further studies to be determined. However, most recent evidence points to LRP1. LRP1 is identified to be the essential receptor for myelin phagocytosis and a mediator of apoE-dependent

neurite outgrowth (Gaultier et al., 2008; Gaultier et al., 2009). Consistently, our preliminary data show that the LRP inhibitor lactoferrin can block the effect of COG112 on LDL uptake by Schwann cells (data not shown here).

In summary, the current study presents a proof of principle that apoE can be a putative target for designing therapeutic interventions for peripheral nerve injuries. The mimetic peptide strategy translates the concept into a potential therapy with demonstrated neurorestorative activities by promoting axonal regeneration and remyelination. These properties are most desirable for a satisfactory functional recovery for peripheral neuropathy.

References

Aono M, Bennett ER, Kim KS, Lynch JR, Myers J, Pearlstein RD, Warner DS, and Laskowitz DT (2003) Protective effect of apolipoprotein E-mimetic peptides on *N*-methyl-D-aspartate excitotoxicity in primary rat neuronal-glial cell cultures. *Neuroscience* **116:**437–445.

Aono M, Lee Y, Grant ER, Zivin RA, Pearlstein RD, Warner DS, Bennett ER, and Laskowitz DT (2002) Apolipoprotein E protects against NMDA excitotoxicity. *Neurobiol Dis* **11:**214–220.

Bain JR, Mackinnon SE, and Hunter DA (1989) Functional evaluation of complete sciatic, peroneal, and posterior tibial nerve lesions in the rat. *Plast Reconstr Surg* **83:**129–138.

Boyles JK, Zoellner CD, Anderson LJ, Kosik LM, Pitas RE, Weisgraber KH, Hui DY, Mahley RW, Gebicke-Haerter PJ, and Ignatius MJ (1989) A role for apolipoprotein E, apolipoprotein A-I, and low density lipoprotein receptors in cholesterol transport during regeneration and remyelination of the rat sciatic nerve. *J Clin Invest* **83:**1015–1031.

Brown CM, Wright E, Colton CA, Sullivan PM, Laskowitz DT, and Vitek MP (2002) Apolipoprotein E isoform mediated regulation of nitric oxide release. *Free Radic Biol Med* **32:**1071–1075.

Chapman J, Vinokurov S, Achiron A, Karussis DM, Mitosek-Szewczyk K, Birnbaum M, Michaelson DM, and Korczyn AD (2001) APOE genotype is a major predictor of long-term progression of disability in MS. *Neurology* **56:**312–316.

Colton CA, Brown CM, Cook D, Needham LK, Xu Q, Czapiga M, Saunders AM, Schmechel DE, Rasheed K, and Vitek MP (2002) APOE and the regulation of microglial nitric oxide production: a link between genetic risk and oxidative stress. *Neurobiol Aging* **23:**777–785.

Corder EH, Saunders AM, Strittmatter WJ, Schmechel DE, Gaskell PC, Small GW, Roses AD, Haines JL, and Pericak-Vance MA (1993) Gene dose of apolipoprotein E type 4 allele and the risk of Alzheimer's disease in late onset families. *Science* **261:**921–923.

Croy JE, Brandon T, and Komives EA (2004) Two apolipoprotein E mimetic peptides, ApoE(130–149) and ApoE(141–155)2, bind to LRP1. *Biochemistry* **43:**7328–7335.

Denny JB (2006) Molecular Mechanisms, Biological Actions, and Neuropharmacology of the Growth-Associated Protein GAP-43. *Curr Neuropharmacol* **4:**293–304.

Fernandez-Valle C, Bunge RP, and Bunge MB (1995) Schwann cells degrade myelin and proliferate in the absence of macrophages: evidence from in vitro studies of Wallerian degeneration. *J Neurocytol* **24:**667–679.

Gao J, Wang H, Sheng H, Lynch JR, Warner DS, Durham L, Vitek MP, and Laskowitz DT (2006) A novel apoE-derived therapeutic reduces vasospasm and improves outcome in a murine model of subarachnoid hemorrhage. *Neurocrit Care* **4:**25–31.

Garbay B, Heape AM, Sargueil F, and Cassagne C (2000) Myelin synthesis in the peripheral nervous system. *Prog Neurobiol* **61:**267–304.

Gaultier A, Arandjelovic S, Li X, Janes J, Dragojlovic N, Zhou GP, Dolkas J, Myers RR, Gonias SL, and Campana WM (2008) A shed form of LDL receptor-related protein-1 regulates peripheral nerve injury and neuropathic pain in rodents. *J Clin Invest* **118:**161–172.

Gaultier A, Wu X, Le Moan N, Takimoto S, Mukandala G, Akassoglou K, Campana WM, and Gonias SL (2009) Low-density lipoprotein receptor-related protein 1 is an essential receptor for myelin phagocytosis. *J Cell Sci* **122:**1155–1162.

Goodrum JF (1991) Cholesterol from degenerating nerve myelin becomes associated with lipoproteins containing apolipoprotein E. *J Neurochem* **56:**2082–2086.

Goodrum JF, Brown JC, Fowler KA, and Bouldin TW (2000) Axonal regeneration, but not myelination, is partially dependent on local cholesterol reutilization in regenerating nerve. *J Neuropathol Exp Neurol* **59:**1002–1010.

Gutman CR, Strittmatter WJ, Weisgraber KH, and Matthew WD (1997) Apolipoprotein E binds to and potentiates the biological activity of ciliary neurotrophic factor. *J Neurosci* **17:**6114–6121.

Handelmann GE, Boyles JK, Weisgraber KH, Mahley RW, and Pitas RE (1992) Effects of apolipoprotein E, beta-very low density lipoproteins, and cholesterol on the extension of neurites by rabbit dorsal root ganglion neurons in vitro. *J Lipid Res* **33:**1677–1688.

Hargreaves K, Dubner R, Brown F, Flores C, and Joris J (1988) A new and sensitive method for measuring thermal nociception in cutaneous hyperalgesia. *Pain* **32:**77–88.

Ignatius MJ, Gebicke-Härter PJ, Skene JH, Schilling JW, Weisgraber KH, Mahley RW, and Shooter EM (1986) Expression of apolipoprotein E during nerve degeneration and regeneration. *Proc Natl Acad Sci USA* **83:**1125–1129.

Ji RR and Suter MR (2007) p38 MAPK, microglial signaling, and neuropathic pain. *Mol Pain* **3:**33.

Kato N, Nemoto K, Arino H, and Fujikawa K (2002) Treatment of the chronic inflammation in peripheral target tissue improves the crushed nerve recovery in the rat: histopathological assessment of the nerve recovery. *J Neurol Sci* **202:**69–74.

Laskowitz DT, Goel S, Bennett ER, and Matthew WD (1997) Apolipoprotein E suppresses glial cell secretion of TNF alpha. *J Neuroimmunol* **76:**70–74.

Laskowitz DT, Thekdi AD, Thekdi SD, Han SK, Myers JK, Pizzo SV, and Bennett ER (2001) Downregulation of microglial activation by apolipoprotein E and apoE-mimetic peptides. *Exp Neurol* **167:**74–85.

Laskowitz DT and Vitek MP (2007) Apolipoprotein E and neurological disease: therapeutic potential and pharmacogenomic interactions. *Pharmacogenomics* **8:**959–969.

Li FQ, Sempowski GD, McKenna SE, Laskowitz DT, Colton CA, and Vitek MP (2006) Apolipoprotein E-derived peptides ameliorate clinical disability and inflammatory infiltrates into the spinal cord in a murine model of multiple sclerosis. *J Pharmacol Exp Ther* **318:**956–965.

Lynch JR, Tang W, Wang H, Vitek MP, Bennett ER, Sullivan PM, Warner DS, and Laskowitz DT (2003) APOE genotype and an ApoE-mimetic peptide modify the systemic and central nervous system inflammatory response. *J Biol Chem* **278:**48529–48533.

Lynch JR, Wang H, Mace B, Leinenweber S, Warner DS, Bennett ER, Vitek MP, McKenna S, and Laskowitz DT (2005) A novel therapeutic derived from apolipoprotein E reduces brain inflammation and improves outcome after closed head injury. *Exp Neurol* **192:**109–116.

Mahley RW (1988) Apolipoprotein E: cholesterol transport protein with expanding role in cell biology. *Science* **240:**622–630.

Mazzer PY, Barbieri CH, Mazzer N, and Fazan VP (2008) Morphologic and morphometric evaluation of experimental acute crush injuries of the sciatic nerve of rats. *J Neurosci Methods* **173:**249–258.

Müller HW, Gebicke-Härter PJ, Hangen DH, and Shooter EM (1985) A specific 37,000-dalton protein that accumulates in regenerating but not in nonregenerating mammalian nerves. *Science* **228:**499–501.

Nathan BP, Bellosta S, Sanan DA, Weisgraber KH, Mahley RW, and Pitas RE (1994) Differential effects of apolipoproteins E3 and E4 on neuronal growth in vitro. *Science* **264:**850–852.

Sheng Z, Prorok M, Brown BE, and Castellino FJ (2008) *N*-Methyl-D-aspartate receptor inhibition by an apolipoprotein E-derived peptide relies on low-density lipoprotein receptor-associated protein. *Neuropharmacology* **55:**204–214.

Singh K, Chaturvedi R, Asim M, Barry DP, Lewis ND, Vitek MP, and Wilson KT (2008) The apolipoprotein E-mimetic peptide COG112 inhibits the inflammatory response to Citrobacter rodentium in colonic epithelial cells by preventing NF-kappa B activation. *J Biol Chem* **283:**16752–16761.

Skene JH and Shooter EM (1983) Denervated sheath cells secrete a new protein after nerve injury. *Proc Natl Acad Sci USA* **80:**4169–4173.

Song XY, Zhou FH, Zhong JH, Wu LL, and Zhou XF (2006) Knockout of p75(NTR) impairs re-myelination of injured sciatic nerve in mice. *J Neurochem* **96:**833–842.

Sorkin LS, Xiao WH, Wagner R, and Myers RR (1997) Tumour necrosis factor-alpha induces ectopic activity in nociceptive primary afferent fibres. *Neuroscience* **81:**255–262.

Vitek MP, Brown CM, and Colton CA (2009) APOE genotype-specific differences in the innate immune response. *Neurobiol Aging* **30:**1350–1360.

Wagner R and Myers RR (1996) Endoneurial injection of TNF-alpha produces neuropathic pain behaviors. *Neuroreport* **7:**2897–2901.

Address correspondence to: Dr. Feng-Qiao Li, 79 TW Alexander Drive, P.O. Box 110606, Research Triangle Park, NC 27709. E-mail: fli@cognosci.com